Electronic and magneto-transport in chirality sorted carbon nanotube films

Dawid Janas[a,*], Nikodem Czechowski[b,c], Zbigniew Adamus[b], Tomasz Giżewski[d]

[a] *Department of Chemistry, Silesian University of Technology, B. Krzywoustego 4, 44-100 Gliwice, Poland*

[b] *Institute of Physics, Polish Academy of Sciences, Aleja Lotnikow 32/46, 02-668 Warsaw, Poland*

[c] *SKA-Polska, Aleje Jerozolimskie 125/127, 00-024 Warsaw, Poland*

[d] *Faculty of Electrical Engineering and Computer Science, Lublin University of Technology, Nadbystrzycka 38A, Lublin, Poland*

Abstract

This research details electronic and magneto-transport in unsorted and chirality-enriched carbon nanotube (CNT) films. By measuring electrical conductivity from 4 K to 297 K we were able to assign the governing mechanism of electronic transport. Fluctuation-Induced Tunnelling was in accordance with the obtained data and very well matched the underlying physics. We demonstrated how a change in the type of CNT to make the film affects its electrical performance. As the temperature was decreased down to cryogenic conditions, up to 56 fold increase in resistance was noted. Moreover, measurement of magnetoresistance (MR) revealed non-monotonic dependence on the applied magnetic field. Initial negative component of MR was eventually overpowered by the positive MR component as the field strength was increased beyond a certain threshold.

Key words: carbon nanotubes; electrical properties; magnetoresistance

Introduction

Nanocarbon materials such as carbon nanotubes (CNTs) and graphene have made a significant impact on a large number of facets of science and technology. Due to their

* Corresponding author. Tel/Fax: +48 32 2372958. E-mail address: dawid.janas@polsl.pl (D. Janas).

remarkable electrical [1-3], thermal [3-5], mechanical [6-8], optical [9-11] and other properties they have been regarded as a viable solution, which can help avoid the limitations of the commonly used materials. Ever since the unprecedented levels of performance have been observed at the nanoscale, the community has put efforts in making macroscale devices from nanocarbon, which would attain similar characteristics. One of the key issues to be addressed to achieve this goal is the problem of largely indiscriminate character of the synthesis. Most methods of CNT manufacture produce mixtures of CNTs of various chiralities [12], which has a deleterious effect on the overall performance of their macroscopic assembly. For instance, chiral angle plays a major role in the electrical character of a given CNT. Depending on the way the conceptual graphene sheet is rolled-up to form a CNT, it can either be semiconducting or metallic. For some applications such as transistors, the presence of metallic CNTs is highly unwanted because they make a short circuit, which deteriorates the performance of the device by significantly decreasing the on/off ratio [13]. On the other hand, CNTs have been envisioned as next generation conductors, which can enhance the technology of copper [14] or even outperform it [15]. In such case the higher the content of metallic CNTs (with their notable electrical conductivity) the better. It is clear that preferential synthesis [16-18] or post-synthetic sorting [19-21] of CNTs should be more widely used not only for reaching a certain level of performance, but, most importantly, for the research to be more precise about the underlying mechanisms under investigation.

In this paper, we demonstrated how a change in the employed CNT type to make a CNT film affects their electronic- and magneto-transport over a wide temperature range (4-297 K). Measurements under cryogenic conditions enabled us to probe the mechanism of electrical conductivity in unsorted and chirality-defined CNT macroscopic materials. Furthermore, a study of magnetoresistance (MR) at low temperature enabled us to validate the mode of electronic transport in these materials.

1. Experimental

Four types of CNTs were used: technical grade Nanocyl NC7000 (NC), CNT carpet produced in house (CPT), (6,5) and (7,6) enriched CoMoCAT SWCNTs procured from SouthWest NanoTechnologies (USA). The first two are composed of multi-wall CNTs (MWCNTs), whereas chirality defined material is based on single-wall CNTs (SWCNTs). Synthesis of CPT was carried out according to a previously published method [22,23]. Toluene (carbon source) and ferrocene (catalyst, 5.5 wt% solution in toluene) mixture was continuously injected (4 mL/h) into a horizontal furnace equipped with a quartz tube. The reaction was run at 760°C under argon (1.8 L_{normal}/min) over the course of 5 hours. After the reaction the product was scraped off quartz reaction tube.

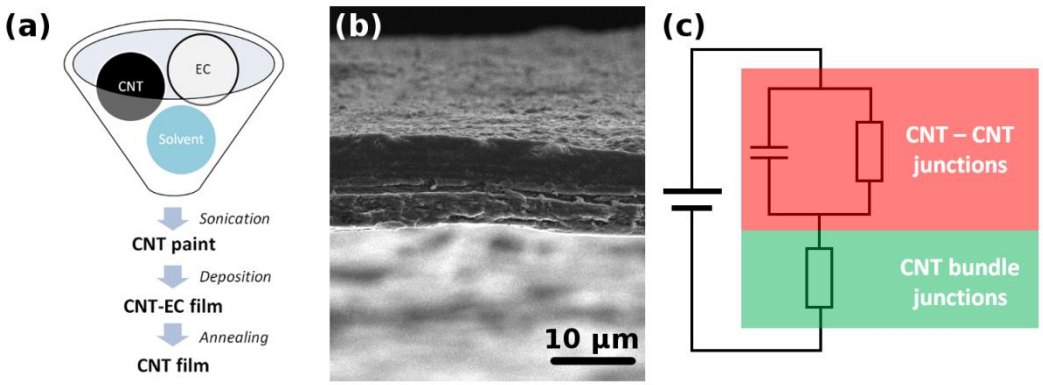

Fig. 1 (a) manufacture of free-standing CNT films, (b) SEM micrograph of CNT film cross-section, (c) equivalent circuit for CNT film

The CNT films were made by a method, which we recently reported [24]. A particular type of CNTs was dispersed in acetone/toluene mixture by ultrasonication by using ethyl cellulose (EC) as stabilizing agent (Fig. 1a). CNT based paint was then deposited onto a Kapton sheet, on which it formed a CNT-EC film. Due to low adhesion of the film to the substrate it could be easily detached from its surface. Finally, EC was removed by flash annealing by igniting the film with a lighter [25]. CNT films (4 aforementioned types) free of polymer were then used for the study.

Transmission Electron Microscopy (TEM, Tecnai F20) was used to probe the microstructure of the material.

Raman spectroscopy (inVia Renishaw Raman microscope, $\lambda = 633$ nm) acquired in the range of 1180 to 1780 cm^{-1} gave information regarding the sample purity (intensity of defect-induced band D was divided by the intensity of the mode of graphitic vibrations G). All spectra were normalized to the intensity of G peak. G modes of (6,5) and (7,6) CNTs split into G- and G+ components, as expected for highly-semiconducting CNTs. In their case, spectra were normalized to G+ mode and I_D/I_{G+} ratio was calculated. For each sample, 10 spectra were collected from different locations and averaged to reach statistical significance.

CNT films were placed in a sample holder with four contacts, allowing for precise electrical measurements. The sample holder was equipped with a semiconductor thermometer to measure its temperature and a heating element to heat the sample.

The sample holder with the investigated CNT film was placed in a helium bath cryostat. The cryostat chamber was evacuated and purged with helium several times in order to keep the sample in contamination-free atmosphere during cooling down. After purging the chamber, samples in the cryostat were cooled down to liquid helium temperature (4.2 K).

The samples were biased with current and the voltage drop was measured, allowing for resistance calculation. After the sample temperature stabilised, the magnetic field was swept from -8.5 T to 8.5 T while the sample resistance was measured. Such measurement of magnetoresistance was carried out at 4.2 K (all samples) and at 50 K (additionally NC). After the magnetoresistance measurements the sample was heated up to room temperature in order to acquire the temperature resistance dependence. Furthermore, I–V curves for the samples were measured at room temperature.

2. Results

2.1.Electronic transport

Electrical properties of individual CNTs are highly dependent on the chiral angle. To investigate how that effect works on the macroscopic scale, CNT films of various CNT types (unsorted and chirality enriched) and purity were manufactured (characterization by TEM and Raman spectroscopy is given in Fig. S1-2). We measured I–V curves at room temperature to obtain their resistance (Fig. 2a), which was on the order of a few Ohms. Variation can be explained by the presence of different CNT types each of which has its own certain ability to transport charge. The CNTs are also of different length, diameter, porosity, alignment and purity what significantly affects junction resistance, which is often predominant in macroscopic objects made of CNTs [26].

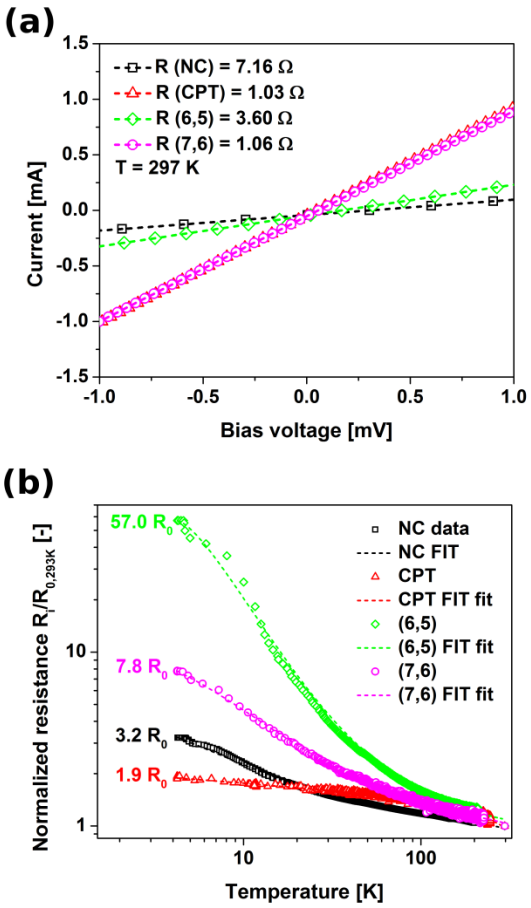

Fig. 2 (a) I–V curves, (b) the influence of temperature on electrical resistance

That is why, in this context it is often more appropriate to quantify CNT electrical behavior using normalized resistance (divided by room temperature measured at 293K), which we will use from this point unless indicated otherwise.

All of the samples showed decrease of resistance with temperature (*dR/dT < 0*) up to 293K, what is indicative of predominantly semiconducting character (Fig. 2b). In none of them the upturn point leading to metallic character regime could be discerned (commonly observed in for instance directly-spun CNT fibers or films [27]). As the temperature is decreased to 4.2K the increase in resistance becomes significant. Unsorted NC and CPT reach only 1.9 R_0 and 3.2 R_0, respectively. Because they have not been subjected to any sorting, but used as-is, the films comprise plenty of metallic CNTs. Resistance of metallic CNTs increases with temperature (*dR/dT > 0*), so the low temperature increase of $R_{4.2K}$ for these two CNT types is much less notable as the semiconducting and metallic influence cancel each other out to some extent. However, each time semiconducting character prevails. In the case of predominantly (7,6) and, even more, (6,5) the increase in resistance is much larger: 7.8 R_0 and 57 R_0, respectively. This is not surprising given the fact that both of these types of CNTs are semiconducting. More significant increase in resistance in the case of (6,5) as compared with (7,6) can be explained by a 10% larger level of enrichment with a particular chirality (as specified by the manufacturer). Even small presence of impurities (such as unwanted CNT type) strongly affects electrical properties – semiconducting performance in particular [28].

Conductivity data was found to fit well with Fluctuation-Induced Tunnelling (FIT) model proposed by Sheng [29] corrected for intrinsic metallic contribution [27]:

$$R(T) = R_{FIT} \exp\left(\frac{T_1}{T_2+T}\right) + BT \quad (1)$$

$T_1 = 8\varepsilon_0\hbar A V_0^2/(e^2 k_B w)$ and $T_2 = 16\varepsilon_0\hbar A V_0^{\frac{3}{2}}/(\pi e^2 k_B (2m_e)^{\frac{1}{2}} w^2)$ wherein A (tunnel junction area), w (its width), V_0 (height of contact potential) [30] and R_{FIT}, B are fitting parameters [27].

In disordered anisotropic materials such as these CNT films, there are long conducting pathways made from individual CNTs of large aspect ratio separated by small insulating barriers, which gives rise to junction resistance. Thermal motion of electrons can tunnel them through these barriers. As described by Terrones *et al.*, transport through such CNT macroassemblies can be considered as dominated by the CNT-CNT capacitance and resistance combined with interbundle resistance component [31]. Equivalent circuit is given in Fig. 1c. Moreover, suitability of the FIT model is also validated by the fact that the slope of resistance approaches zero and tends to saturate at a finite value [27,32]. There are also other reports, which prove its appropriateness for CNT films or fibers [30,33].

It is important to note that fitting Variable Range Hopping (VRH) models failed for all dimensionalities. The results are presented in the Supplementary information file (Fig. S3-S6).

$$R(T) = R_0 \exp\left(\frac{T_M}{T}\right)^{1/(d+1)} \quad (2)$$

R_0 (room temperature resistance), M (Mott temperature), d (dimensionality, d=1–3 for 1D–3D VRH).

2.2.Magneto-transport

Measurement of magnetoresistance (MR) from -8.5 T to 8.5 T at 4.2K enabled us to note only negative MR component for unsorted CNT films (Fig. 3a,b), but chirality-enriched CNT films of strongly semiconducting character revealed also the positive MR component (Fig. 3c,d). Furthermore, decrease in normalized resistance reaches about 10% (unsorted CNT films), while the same effect is much less pronounced for more homogeneous (6,5) and (7,6) CNT films, for which a decrease of 3% was evident up to the upturn point. Non-monotonic relation between MR and T was observed for CNT macroscopic assemblies before [30,33-35]. However, most of the time electronic transport modelling was though to follow VRH.

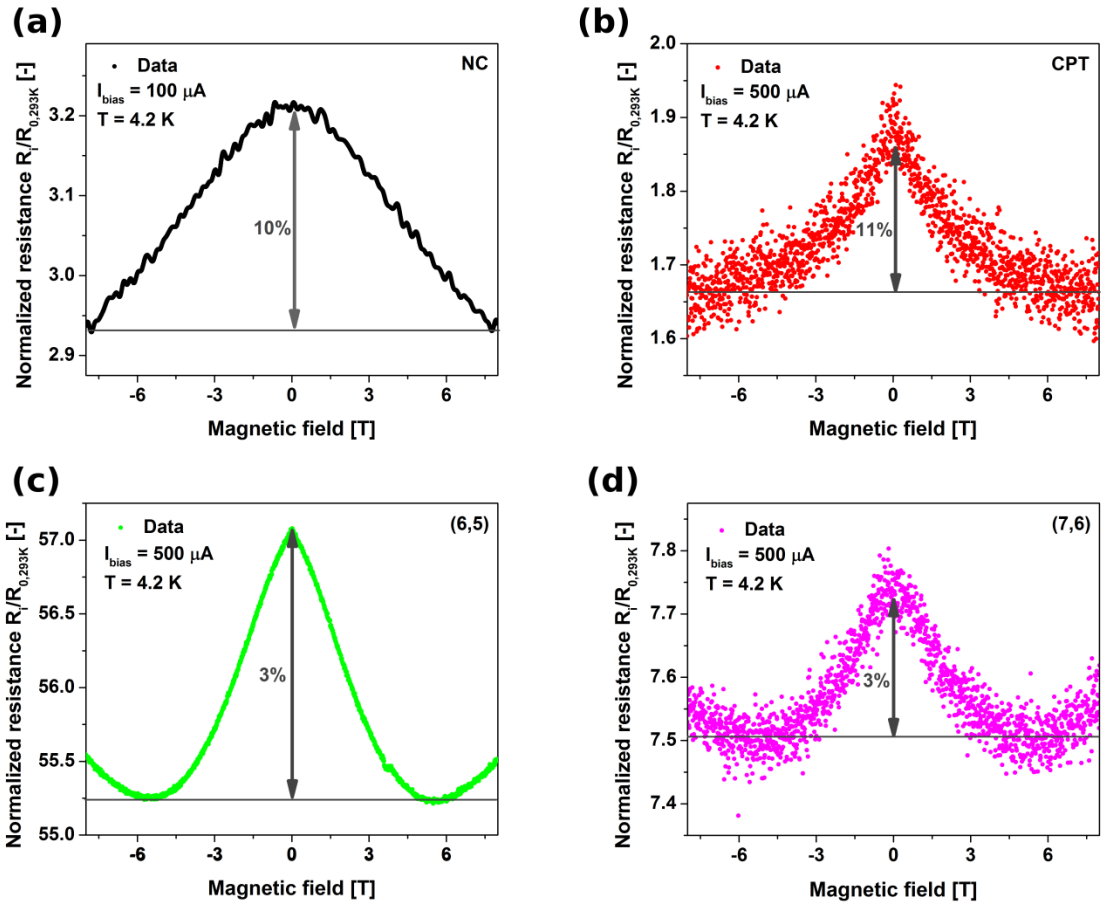

Fig. 3 Magnetoresistance in CNT films based on (a) NC, (b) CPT, (c) (6,5) and (d) (7,6) CNTs.

The theoretical model of MR for FIT mechanism (particularly for CNTs) is not well established [30,36,37]. In a MR study of fine graphite powders, wherein electronic transport was also described by FIT, the origin of negative MR component was ascribed to an interplay of the effects of level crossing and shifting [38]. What regards the positive MR component, shrinkage of electron wave functions was given as a possible underlying reason for this effect [30,38]. We were able to model the dependence of MR on the applied magnetic field B for all the CNT films by using the following relation valid for weak magnetic fields (Fig. S7)[39] :

$$\ln\left(\frac{R(T)}{R_0}\right) = A_0 - A_{\frac{1}{2}}\sqrt{B} + A_2 B^2 \qquad (3)$$

A_0, $A_{1/2}$ – coefficients of negative MR component, A_2 – coefficient of positive MR component

It has been reported that fullerenes (K_xC_{70} [40,41], K_3C_{60} [42]) and SWCNTs[39] can show predominantly negative MR at low H ($B \propto H^2$) and upturn to positive MR at high H ($B \propto H^{1/2}$). However, to the best of our knowledge, this behaviour has not been shown before to be valid for CNTs conducting by fluctuation-induced tunnelling, which is the case here.

Moreover, while working on CNT films, Baumgartner *et al.* reported that their negative MR component decreased with temperature because the surface of phase coherent loops of equivalent paths was reduced as more backflow was induced by thermal energy [33]. Our results also showed that increase in temperature from 4.2 K to 50 K decreased the negative MR component by more than 50% (Fig. 4). MR data seems to support FIT transport in these CNT films.

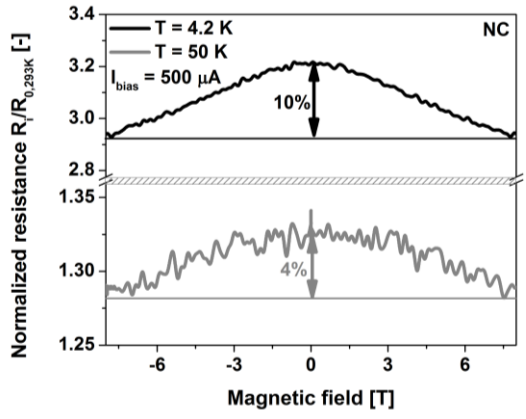

Fig. 4 The influence of temperature on magnetoresistance

3. Conclusions

We presented the results of investigation electronic- and magneto-transport in unsorted and chirality-enriched CNT films produced in house. The results showed that, contrary to many other reports, the electrical conductivity in 4 – 300K range does not follow the mechanism of Variable Range Hopping regardless of its dimensionality. Instead, Fluctuation-Induced Tunnelling was able to model the observed behaviour. The data from magnetoresistance study under cryogenic conditions was in accordance with the proposed mode of transport. We showed that the same mechanism of charge transport was valid for all the CNT film types

regardless of their purity or dominant chirality, but the materials showed obvious differences in the magnitude of negative and positive components of magnetoresistance. In the case of unsorted CNT films, the upturn point from negative to positive MR could not be discerned in the selected magnetic field window. More research is needed to pinpoint the theory how exactly these materials conduct depending on the type of CNTs employed. Greater insight on this front would enable design and manufacture of CNT electronic devices better tailored for specific applications.

4. Acknowledgements

D.J. thank National Science Center, Poland (under the Polonez program, grant agreement UMO-2015/19/P/ST5/03799) and the European Union's Horizon 2020 research and innovation programme (Marie Skłodowska-Curie grant agreement 665778). D.J. would also like to acknowledge Foundation for Polish Science for START scholarship (START 025.2017) and the Rector of the Silesian University of Technology in Gliwice for funding the research in the framework of habilitation grant (04/020/RGH17/0050). N.C. would like to acknowledge National Science Center, Poland support under Fuga program, grant agreement UMO-2015/16/S/ST3/00477.

References

1 G. J. Brady, A. J. Way, N. S. Safron, H. T. Evensen, P. Gopalan, and M. S. Arnold, Science Advances **2** (2016).

2 J. Sandler, M. S. P. Shaffer, T. Prasse, W. Bauhofer, K. Schulte, and A. H. Windle, Polymer **40,** 5967 (1999).

3 C. Teng, D. Xie, J. Wang, Z. Yang, G. Ren, and Y. Zhu, Advanced Functional Materials **27,** 1700240 (2017).

4 K. K. Koziol, D. Janas, E. Brown, and L. Hao, Physica E: Low-dimensional Systems and Nanostructures **88,** 104 (2017).

5 A. A. Balandin, S. Ghosh, W. Bao, I. Calizo, D. Teweldebrhan, F. Miao, and C. N. Lau, Nano Letters **8,** 902 (2008).

6 D. Hu, Y. Xing, M. Chen, B. Gu, B. Sun, and Q. Li, Composites Science and Technology **141,** 137 (2017).

7 B. Arash, H. S. Park, and T. Rabczuk, Composites Part B: Engineering **80,** 92 (2015).

8 D. Akinwande, C. J. Brennan, J. S. Bunch, P. Egberts, J. R. Felts, H. Gao, R. Huang, J.-S. Kim, T. Li, Y. Li, K. M. Liechti, N. Lu, H. S. Park, E. J. Reed, P. Wang, B. I. Yakobson, T. Zhang, Y.-W. Zhang, Y. Zhou, and Y. Zhu, Extreme Mechanics Letters **13,** 42 (2017).

[9] S. M. Bachilo, M. S. Strano, C. Kittrell, R. H. Hauge, R. E. Smalley, and R. B. Weisman, Science **298,** 2361 (2002).
[10] S. Kruss, A. J. Hilmer, J. Zhang, N. F. Reuel, B. Mu, and M. S. Strano, Advanced Drug Delivery Reviews **65,** 1933 (2013).
[11] L. A. Falkovsky, Journal of Physics: Conference Series **129,** 012004 (2008).
[12] D. Janas, Materials Chemistry Frontiers (2017).
[13] C. Qiu, Z. Zhang, D. Zhong, J. Si, Y. Yang, and L.-M. Peng, ACS Nano **9,** 969 (2015).
[14] D. Janas and B. Liszka, Materials Chemistry Frontiers (2017).
[15] S. Hong and S. Myung, Nat Nano **2,** 207 (2007).
[16] J. R. Sanchez-Valencia, T. Dienel, O. Groning, I. Shorubalko, A. Mueller, M. Jansen, K. Amsharov, P. Ruffieux, and R. Fasel, Nature **512,** 61 (2014).
[17] S. M. Bachilo, L. Balzano, J. E. Herrera, F. Pompeo, D. E. Resasco, and R. B. Weisman, Journal of the American Chemical Society **125,** 11186 (2003).
[18] B. Liu, J. Liu, X. Tu, J. Zhang, M. Zheng, and C. Zhou, Nano Letters **13,** 4416 (2013).
[19] C. Y. Khripin, J. A. Fagan, and M. Zheng, Journal of the American Chemical Society **135,** 6822 (2013).
[20] H. Liu, D. Nishide, T. Tanaka, and H. Kataura, **2,** 309 (2011).
[21] M. S. Arnold, A. A. Green, J. F. Hulvat, S. I. Stupp, and M. C. Hersam, Nat Nano **1,** 60 (2006).
[22] S. Boncel, S. W. Pattinson, V. Geiser, M. S. P. Shaffer, and K. K. K. Koziol, Beilstein Journal of Nanotechnology **5,** 219 (2014).
[23] C. Singh, M. Shaffer, I. Kinloch, and A. Windle, Physica B: Condensed Matter **323,** 339 (2002).
[24] D. Janas, M. Rdest, and K. K. K. Koziol, Materials & Design **121,** 119 (2017).
[25] D. Janas and G. Stando, Scientific Reports **7,** 12274 (2017).
[26] D. Janas and K. K. Koziol, Nanoscale **8,** 19475 (2016).
[27] J. S. Bulmer, T. S. Gspann, F. Orozco, M. Sparkes, H. Koerner, A. Di Bernardo, A. Niemiec, J. W. A. Robinson, K. K. Koziol, J. A. Elliott, and W. O'Neill, Scientific Reports **7,** 12977 (2017).
[28] G. S. Tulevski, A. D. Franklin, and A. Afzali, ACS Nano **7,** 2971 (2013).
[29] P. Sheng, Physical Review B **21,** 2180 (1980).
[30] V. K. Ksenevich, V. B. Odzaev, Z. Martunas, D. Seliuta, G. Valusis, J. Galibert, A. A. Melnikov, A. D. Wieck, D. Novitski, M. E. Kozlov, and V. A. Samuilov, Journal of Applied Physics **104,** 073724 (2008).
[31] J. Terrones, J. A. Elliott, J. J. Vilatela, and A. H. Windle, ACS Nano **8,** 8497 (2014).
[32] W. Zhou, J. Vavro, C. Guthy, K. I. Winey, J. E. Fischer, L. M. Ericson, S. Ramesh, R. Saini, V. A. Davis, C. Kittrell, M. Pasquali, R. H. Hauge, and R. E. Smalley, Journal of Applied Physics **95,** 649 (2003).
[33] G. Baumgartner, M. Carrard, L. Zuppiroli, W. Bacsa, W. A. de Heer, and L. Forró, Physical Review B **55,** 6704 (1997).
[34] G. T. Kim, J. G. Park, Y. W. Park, K. Liu, G. Düsberg, and S. Roth, Synthetic Metals **103,** 2551 (1999).
[35] J. S. Bulmer, A. Lekawa-Raus, D. G. Rickel, F. F. Balakirev, and K. K. Koziol, Scientific Reports **7,** 12193 (2017).
[36] V. Ksenevich, T. Dauzhenka, D. Seliuta, I. Kasalynas, T. Kivaras, G. Valusis, J. Galibert, R. Helburn, Q. Lu, and V. Samuilov, physica status solidi (c) **6,** 2798 (2009).
[37] Q. Lu, V. Samuilov, V. Ksenevich, T. Dauzhenka, and R. S. Helburn, in *Interfaces and Interphases in Analytical Chemistry*; *Vol. 1062* (American Chemical Society, 2011), p. 185.
[38] A. B. Pakhomov, X. X. Zhang, H. Liu, X. R. Wang, H. J. Huang, and S. H. Yang, Physica B: Condensed Matter **279,** 41 (2000).
[39] S. V. Demishev, A. D. Bozhko, V. V. Glushkov, E. A. Kataeva, A. G. Lyapin, E. D. Obraztsova, T. V. Ishchenko, N. A. Samarin, and N. E. Sluchanko, Physics of the Solid State **50,** 1386 (2008).
[40] Z. H. Wang, K. Ichimura, M. S. Dresselhaus, G. Dresselhaus, W. T. Lee, K. A. Wang, and P. C. Eklund, Physical Review B **48,** 10657 (1993).

[41] Z. H. Wang, M. S. Dresselhaus, G. Dresselhaus, K. A. Wang, and P. C. Eklund, Physical Review B **49,** 15890 (1994).
[42] Z. H. Wang, A. W. P. Fung, G. Dresselhaus, M. S. Dresselhaus, K. A. Wang, P. Zhou, and P. C. Eklund, Physical Review B **47,** 15354 (1993).